Chem Rev Lett 9 (2026) 322-332

Research Article

Chemical Review and Letters
journal homepage: www.chemrevlett.com
ISSN (online): 2645-4947 (print) 2676-7279

Invitro applications of some novel Metallo-Mannich bases based on acyclovir: Antimicrobial and antioxidant activity

Tabarak J. Ahmed[1], Mahasin F. Alias[1,*]

[1]*Department of Chemistry, College of Science for Women, University of Baghdad. Iraq.*

ARTICLE INFO

Article history:
Received 21 May 2025
Received in revised form 30 June 2025
Accepted 14 July 2025

Keywords:
Acyclovir
Antimicrobial
Antioxidant
Mannich base
Spectral data

ABSTRACT

This study investigates the novel synthesis of Mannich base complexes, including V(IV), Ru(III), Pt(IV), and Au(III), which are produced from the Acyclovir-Mannich base. All structures of these novel compounds were described using spectroscopic approaches, including ^{1}H,^{13}C-NMR, UV-Vis, mass spectrometry, FTIR, metal, and elemental analysis, in addition to magnetic susceptibility and conductivity measurements. The diagnosis found that the VO-complex possesses a square pyramidal geometry, the Au-complex exhibits square planar geometry, and the Ru and Pt complexes are octahedral. All synthesized compounds were subjected to the antioxidant assay. The antioxidant activity indicates that the Ru (III) complex exhibited superior antioxidant efficacy compared to the others. The value of IC_{50} concerning this combination was 311.50 µg/ml. The study also involves evaluating the efficacy of these compounds in inhibiting the bacteria *Acinetobacter baumannii*, a Gram-negative, and *Streptococcus pyogenes*, a Gram-positive, as well as their antifungal activity against the microorganism *Candida albicans*, utilizing two separate concentrations (50 and 100) mg/ml. The data indicate that higher concentrations enhance antibacterial and antifungal action, and the Pt-complex exhibits more synergistic effectiveness and demonstrates excellent antibacterial properties against *Streptococcus pyogene*s.

1. Introduction

Heterocyclic, particularly nitrogen-containing, compounds play key roles in biologically active pharmaceuticals; therefore, their synthesis has attracted significant research interest [1,2]. Mannich bases, recognized as beta-amino ketones, are considered a significant category of compounds in medicinal chemistry. Mannich reactions represent essential and pivotal carbon-carbon bond-forming processes in organic synthesis [3]. Mannich bases are formed via the condensation reaction involving active hydrogen-containing compounds, aldehydes, and secondary amines, creating three unique products. The formation of these Mannich base products is affected by the substrate's nucleophilicity and the reaction medium's pH [4]. There is an urgent need to synthesize novel antimicrobial drugs that demonstrate strong efficacy against drug-resistant microbes [5].

Because the amino group can be readily converted into a variety of other functionalities, the chemistry of the amino alkylation of aromatic substrates by the synthesis and modification of physiologically active molecules with physical, chemical significance, and physiological characteristics are highly desirable applications for the Mannich process [6]. A practical method for incorporating a basic amino-alkyl chain into various medications and substances is through the Mannich reaction [7]. In chemical studies, metal complexes of Mannich bases have attracted significant interest because of their exceptional ligand selectivity and responsiveness to different metal ions [8,9]. Acyclovir or (2-amino-1,9-dihydro-9-((2-hydroxy ethyl)methyl)-6H-purin-6-one), chemically known as acycloguanosine, is an antiviral drug that serves as a guanosine analog [10]. Recently, the study of the coordination capabilities of synthetic Mannich bases has gained significant attention due to their medicinal uses as antiviral, antimicrobial, and anticancer drugs [11].

Two studies were used Ganciclovir (Acyclovir analogue) to prepare different Mannich bases. The first study was published in 2012 by Joshi S. *et al*. [12] and

* Corresponding author E-mail: mahasinfa_chem@csw.uobaghdad.edu.iq
https://doi.org/10.22034/crl.2025.525296.1607

included the preparation of ten Mannich bases derived from Ganciclovir with different sulphonamides and secondary amines. These newly Mannich bases were characterized and by ^{1}HNMR, IR, UV.-VIS, XRD and SEM, as well as, tested as antibacterial versus (*P.aeruginosa*, *K.pneumoniae*, and *S.typhi*) and showed interesting results using concentrations [80, 160, 320] mg/mL. In 2017, Joshi S. and co-workers were screened these Mannich bases against other microbes (*E. coli*, *S. aureus* and *B. subtilis*) under same concentrations in the study [13].

In general, the results were showed more potential vs. (*E. coli*, *S. aureus* and *B. subtilis*) than (*P.aeruginosa*, *K.pneumoniae*, and *S.typhi*).

In this work, the acyclovir drug was used to derived a new Mannich base and used it as chelator to synthesized different metal complexes and predict their medicinal effects by studying some of their *in-vitro* application as antimicrobe and antioxidation activities.

2. Materials and Methods

2.1. Materials and Instruments

The study utilized the following chemicals and reagents: acyclovir, morpholine, metal chlorides, methanol, ethanol, and formaldehyde. The UV-Vis spectra in DMSO were obtained with a Shimadzu UV-1601 spectrophotometer (Shimadzu Company; Tokyo, Japan). The Fourier transform infrared (FTIR) spectra were obtained with the FT-IR 8300 Shimadzu spectrophotometer, covering the 4000-200 cm^{-1} (Shimadzu Corporation; Tokyo, Japan). Melting points were investigated using open glass capillaries. Metal content measurements were performed at the Research and Technology Center of Environment, Water and Renewable Energy of the Authority of Scientific Research using the flame system of atomic absorption spectrophotometry (AAS), specifically the Shimadzu 760 model, Japan. Magnetic sensitivity measurements were obtained using the auto magnetic susceptibility Balance-Sherwood Scientific Ltd (UK) at Al-Mustansiriyah University. Conductivity measurements were conducted utilizing a Corning conductivity meter 220, carried out in a DMSO solvent at a concentration of (10^{-3} M). The elemental analyses (C.H.N.S.) were obtained using EA-034.mth. Mass spectra were recorded using the DIRECT PROBE at the Agilent USA Central Lab of the University of Tehran.

2.2. Synthesis of Mannich Base

To prepare ligand (L) of Mannich Base from (0.225g, 0.01 mole) Acyclovir and (0.087, 0.01 mole) morpholine, the starting materials were dissolved in 30 ml of ice-cold methanol in a beaker with constant shaking. Then, formaldehyde (0.03g, 0.01 mole) was slowly added to the same solution, heated to reflux for about three hrs., and then frozen overnight. The white precipitate was obtained, washed, and recrystallized from ethanol [14], (Scheme 1).

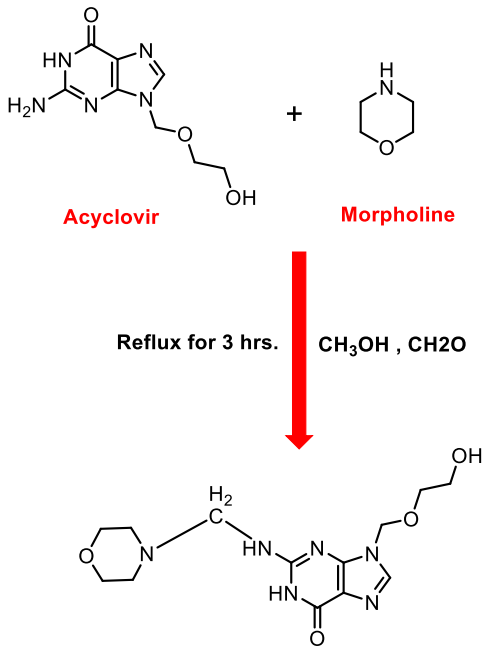

Scheme 1. Synthetic pathway of acyclovir-Mannich base.

2.3. Synthesis of Complexes

The complexes were synthesized by the reaction of equal molar ratio of Metal to ligand, (0.324g, 0.001 mole) of L with (0.001 mole) of each of these salts: [$VOSO_4 \cdot H_2O$ (0.180 g), $H_2PtCl_6 \cdot 6H_2O$ (0.517 g), $HAuCl_4 \cdot H_2O$ (0.357 g), and $RuCl_3$ (0.207 g)]. Both the ligand and the metal salt were dissolved separately in 25 ml of ethanol and then mixed together. The combination was refluxed for (2 to 3) hrs., during which the solution's color was altered. The color change is probably because of the formation of the metal complex. Following the reflux, the combination is removed to produce a colored precipitate, which is recrystallized from ethanol for purification and finally dried in a desiccator to obtain powdered metal complexes.

2.4. Antibacterial Activity

The agar well diffusion technique was used to evaluate the MIC concentration's antibacterial activity [15]. Every studied bacterial isolate was developed in nutrient broth and incubated at 37 ºC for 18-24 hrs. After the incubation period, 0.1 ml from each bacterial suspension was uniformly distributed over the surface of nutrient agar and incubated for 24 hrs. at 37 ºC. Using a sterile cotton swab, a colony was hosted in a test tube along with 5 milliliters of normal saline. This produced a bacterial suspension that displayed mild turbidity,

comparable to the standard turbidity solution, which was around 1.5 x 10^8 colony-forming units per milliliter and was thereafter equally distributed over Mueller- Hinton agar medium and let to incubate for 10 minutes. Wells of five millimeters in diameter were formed in the preceding agar layer, with three wells allocated to each plate. Removing the agar discs, 50µl of the solution was dispensed into all wells by a micropipette. Plates were incubated for 18 hrs. at 37 ºC. Subsequently, the diameters of the inhibitory zones were measured.

2.5. Antioxidant Activity

The stable free-radical DPPH had a scavenging effect on radicals, and the method was evaluated for the antioxidant efficacy of vitamin C. 1ml of the normal or diluted solution (500, 250, 125, 62.5, 31.2, 15.6) µg/ml was added to 1ml of the DPPH solution in a test tube. Following a one-hour incubation at 37°C, the absorbance of each solvent was assessed at 517 nm with a spectrophotometer. The ability to scavenge DPPH was evaluated through three separate experiments using Eq. 1 [16].

$$I\% = [(\text{Absblank} - \text{Abssample})/\text{Absblank}] \times 100 \quad (1)$$

Abs sample symbolizes the absorption of the tested compound, whereas Abs $_{blank}$ signifies the control reaction's absorbance, including all reagents except the test compound. The DPPH-scavenging activity was graphed against sample concentration to get the IC_{50}, indicating the absorbance values for each produced molecule.

3. Results and Discussion

3.1. Characterizing the Ligand and its Metal Complexes

Table 1 presents data that elucidate the physical properties of ligand (L) and its complexes, aligning well with the measured values. The proposed molecular structure is developed following characterization through subsequent spectral, conductivity, and magnetic moment analysis.

3.2. FTIR Spectra Analysis

The FT-IR spectrum of the ligand Mannich base (L), shown in (Fig. 1 Supp.), presents some challenges due to overlapping regions among several groups; however, a selection of bands has been made to illustrate the intricate nature of the spectrum. The main IR bands of the free ligand with the metal complexes of the ligand are illustrated in Table 2. The ligand spectrum displays stretching frequencies of ν(CH_2-N) and ν(C=N) at 2923 and 2898 cm^{-1}, as well as 1656 and 1602 cm^{-1}, respectively. Additional bands observed at 3392, 1687, 1361, and 1122 cm^{-1} are attributed to the stretching frequencies of νOH (alcoholic), C=O, ν NCN, and ν CNC, respectively [17]. The FTIR spectrum of the complexes shows the bands of νOH (alcoholic), νNH (amide), νC=O, νC=N, νCOC, δNH (amide), and νC-OH. These bands did not change in position or relative intensity when the coordination with metal ions occurred. This suggests a lack of coordination with metals via the bands previously discussed. In complexes, the bands attributed to the ν (CH_2-N) and ν(NCN) of the previously mentioned ligands shifted to higher wave numbers, with changes in intensity ranging from approximately 12 to 41 cm^{-1}. Equally, the band corresponding to the ν(CNC) of the morpholine ring moved to a low frequency, with intensity changes in the complexes of about 15 to 21 cm^{-1}. This demonstrates coordination via these groups' donor (N, N) atoms. Weaker absorption bands are detected at frequencies under 500 cm^{-1}. Those bands indicate the coordination bonds ν(M-N) formed that connect a metal ion and the nitrogen atom of the Mannich base derivative. A weak band is also observed around 400 cm^{-1}, suggesting the coordination ν(M-O) of the oxygen atom of water with the metal ion [18]. The spectra of the Ru(III), Pt(IV), and Au(III) complexes also displayed a new weak band at a frequency within the range of 317-335 cm^{-1}, which is attributed to the stretching frequency of (M-Cl) [19]. The coordination of the δH_2O band with the central metal ion (aqua) in (Ru, Au, and Pt) complexes varied between (900-800) cm^{-1}[20]. Table 2 presents additional bands. FTIR spectra were shown in the (Fig. 1-5 Supp.).

3.3. Mass Spectroscopy

The mass spectrum functions as a technique for determining synthesized compounds' molecular weight and identifying the studied compounds' fragmentation patterns. The mass spectrum of the prepared ligand and vanadyl complex, illustrated in Figure 2 and 3, is closely equivalent to the proposed structural formula. The spectrum of the ligand revealed the $C_{13}H_{20}N_6O_4$ bands, with one band corresponding to the molecular ion, which was detected at 325.1 m/z for the ligand and 486.9 m/z for V-L. The mass spectra for the ligand and its vanadyl complex displayed additional distinct peaks that resulted from successive fragmentation.

3.4. ^{1}H, ^{13}C-NMR Spectra

The ^{1}HNMR spectrum of the (L) depicted in (Fig. 6 Supp.) reveals proton peaks at 2.5 ppm, which can be attributed to the solvent protons present in DMSO-d_6. The ^{1}HNMR spectrum of the ligand exhibits a signal peak at 2.84 ppm, indicative of the NH moiety. Additionally, the spectrum reveals proton bands at 3.4 and 3.55 ppm, corresponding to the CH_2 groups of Acyclovir. The peak demonstrating a chemical shift within the range of (4.69-4.72) ppm is ascribed to the CH_2-N groups

characteristic of Mannich bases found in the ligand. Other peaks corresponding to specific functional groups are illustrated in Table 3. (Fig. 7 Supp.) presents the ^{13}C-NMR spectrum ligand of [L] in DMSO-d_6 solvent. The chemical shifts observed at 64.39 ppm are attributed to the carbon atoms of the Mannich base. The other groups were detailed in Table 3 [14,19].

Table 1. Physical properties of the ligand and its metal complexes.

Compd.	Color	Melting point ºC	Yield%	M.Wt g/mol	Elemental analysis Found (cal.)			Metal% Found (cal.)	Suggested formula
					C	*H*	*N*		
L	White	238-240	88	324.8	47.5 (48.1)	5.5 (6.1)	26.7 (25.9)	-	$C_{13}H_{20}N_6O_4$
V-L	Olive Green	260> d	82	504.9	29.5 (30.8)	5.2 (4.3)	17.1 (16.6)	11.2 (10.0)	$[VOSO_4L]H_2O$
Ru-L	Brown	209-211	90	603.2	26.5 (25.8)	3.5 (4.6)	14.3 (13.9)	17.2 (16.7)	$[RuLCl(H_2O)_3]Cl_2H_2O$
Pt-L	Yellowish Orang	122-124	80	679.2	21.5 (22.9)	4.2 (3.8)	13.2 (12.3)	29.1 (28.7)	$[PtLCl_2(H_2O)_2]Cl_2H_2O$
Au-L	Yellow	158-160	92	645.1	25.2 (24.1)	4.3 (3.4)	12.8 (13.0)	31.2 (30.5)	$[AuLCl_2]Cl\ H_2O$

d = decomposition degree.

Table 2. Chosen diagnosis FT-IR absorption bands of ligands and complexes.

Com.	νOH	νNH amide	νCH_2 alp.	νCH_2-N	νC=O	νC=N	νCNC morph.	νNCN	δNH amide	νC-OH	νM-N	νM-O	Others
L	3392	3163	3095-2761	2923 2898	1687	1687 1602	1122	1361	1541	1008	---	--	--
VL	3406	3165	2935-2752	2935 2869	1685	1654 1605	1107	1390	1541	1030	534	445	V=O=9755 SO_4=1107 νH_2O=3438 δH_2O=823
RuL	3397	3161	3056-2764	2945 2800	1688	1654 1600	1107	1351	1542	1040	557	451	Ru-Cl=325 νH_2O=3367-3504 δH_2O=891
Pt L	3399	3166	3083-2766	2958 2883	1687	1645 1600	1101	1371	1541	1035	553	466	Pt-Cl=317 νH_2O=3377-3364 δH_2O=827
AuL	3388	3164	3089-2758	2964 2845	1690	1655 1606	1105	1375	1543	1010	534	--	Au-Cl=335 νH_2O=3426 δH_2O=844

Table 3. ^{1}H,^{13}C-NMR spectra data of Ligand.

Symbol	^{1}HNMR, δ(ppm)	^{13}CNMR, δ(ppm)	Functional group
a	5.36,5.40	-	OH $_{aliphatic}$
b	3.55	60.36	CH_2 $_{aliphatic}$
b′	3.47	72.49	CH_2-O $_{aliphatic}$
c	5.90	70.83	N-CH_2
d	7.38,7.86	138.24	CH=N
e	-	151.89	N-C-N
f	-	116.91	C-C-N
g	-	157.29	C=O
h	10.66	-	NH
i	-	154.31	N-C=N
j	2.84	-	NH
k	4.69-4.72	64.39	CH_2-$N_{Mannich\ group}$
l	2.40,2.49	52.93	CH_2-$N_{Morpholine}$
m	3.58	67.01	CH_2-$O_{Morpholine}$

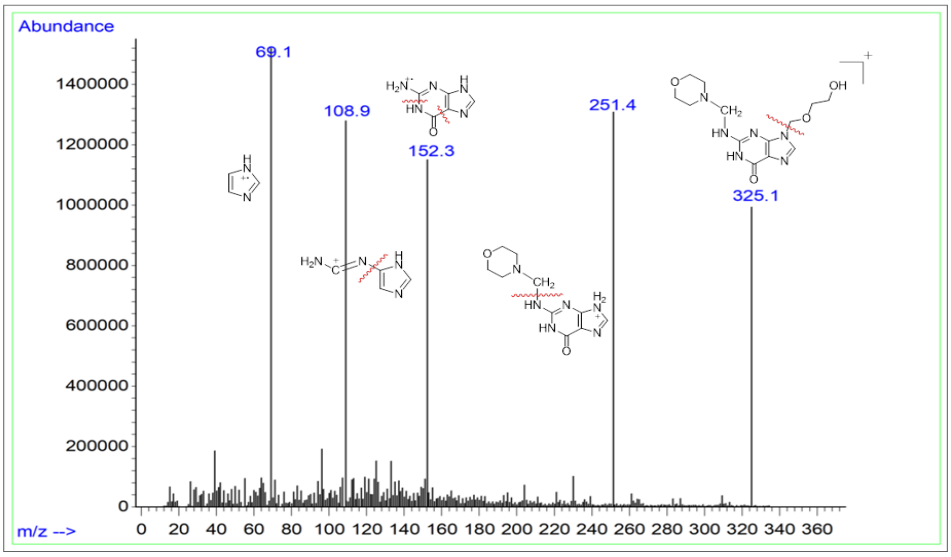

Fig. 2. Mass spectrum of ligand (L).

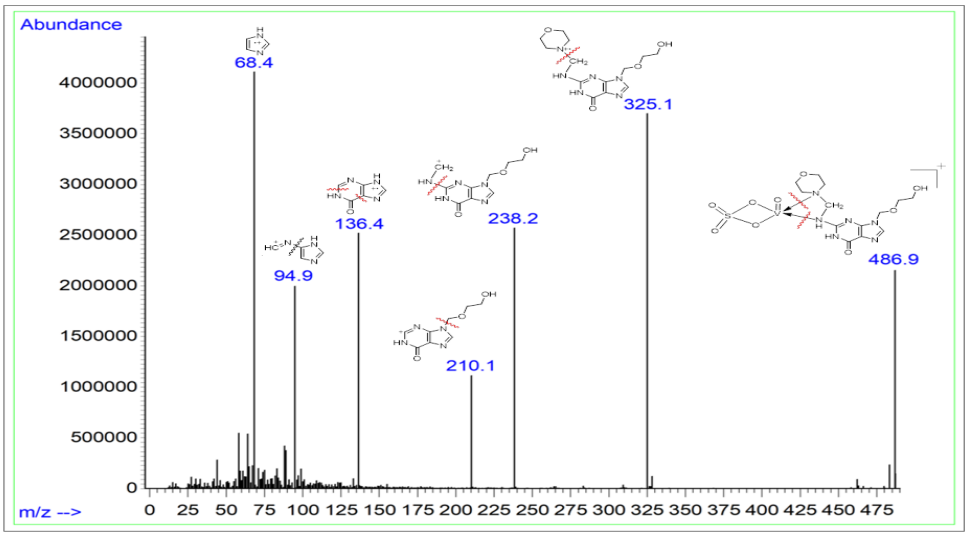

Fig. 3. Mass spectrum of VO-L complex

3.5. Electronic Spectral, Conductivity, and Magnetic Moment

The electronic spectral analyses of the ligand and its complex were performed in DMSO solvent. The Electronic spectrum of the Mannich base ligand, as revealed in Figure 4, typically revealed four main bands. The initial and subsequent absorption bands were observed at 31347, 35714, and 39215 cm^{-1}, attributed to the inter-ligand (n→π*) transition involving the carbonyl, morpholine, and Mannich base. The third and fourth absorption bands at 47619 cm^{-1} are due to the (π→π*) electronic transition of the carbonyl group, purine, and aromatic rings [21].

The olive green electronic spectrum of the Vanadyl complex, Figure 5, displayed four bands at (11961, 14992, 23809, and 37037) cm^{-1}, which are allocated to transitions $^2B_2 \rightarrow {}^2E$, $^2B_2 \rightarrow {}^2B_1$, $^2B_2 \rightarrow {}^2A_1$ and L→V (CT) respectively [22]. The magnetic moment of the existing complex is (2.01 BM). This result indicates the paramagnetic properties of the complex and agrees with the square pyramidal structure [23]. The conductivity evaluation in DMSO indicated that the complex is a non-electrolyte [24].

The ultraviolet-visible spectrum of the brown Ru(III) complex, Figure 6, exhibited three bands at 12800 and 15380 cm^{-1}, corresponding to the transitions $^2T_2g \rightarrow {}^4T_1g$, $^2T_2g \rightarrow {}^4T_2g$, and L→Ru (CT) respectively [25]. The Racah parameter B was determined by fitting the ratio ν_2/ν_1 to the Tanabe-Sugano diagram for the octahedral d5. The Dq/B ratio is 4.5, indicating that B` equals 555 cm^{-1}. The constant field splitting value, Dq, is 2497 cm^{-1}, resulting in a value of 10Dq equal to 24975 cm^{-1}. The third transition underwent theoretical calculations via the Equation 2 :

$$15B` = \nu_3 + \nu_2 - 3\nu_1 \quad (2)$$

with a value determined to be 31345 cm^{-1} [26]. The conductivity measurement indicated that the complex is a

conductor; thus, the two (Cl^{-1}) ions are situated outside the coordination zone. Based on the earlier spectral results and the current findings, the suggested structure is octahedral. The electronic spectrum of the synthesized yellowish-orange Pt(IV) complex, as shown in Figure 7, displayed four bands at 11001, 28571, 37593 cm^{-1}, which are attributed to the transitions $^1A_1g \rightarrow {}^3T_1g + {}^3T_2g$, $^1A_1g \rightarrow {}^1T_1g$, $^1A_1g \rightarrow {}^1T_2g$ and L→Pt (CT) [27]. The magnetic moment of the Pt(IV) complex, characterized by a d^6 configuration, is 0.0 BM.

This result indicates diamagnetism and aligns with the octahedral shape [28].The conductivity measurement demonstrated that the complex is a conductor, implying that the location of the two Cl^{-1} ions is outside the coordination zone. Based on the data and spectroscopy techniques, along with the results obtained, it is proposed that the octahedral structure was synthesized for this complex.

UV-vis spectrum of yellow Au(III) complex, Figure 8, displayed two bands at (30303 and 37735) cm^{-1}, corresponding to the transitions $^1A_1g \rightarrow {}^1B_1g$, $^1A_1g \rightarrow {}^1Eg$, respectively. Additionally, another band appeared at 24783 cm^{-1}, which may be attributed to the L→Au (CT) transition [29].

The magnetic moment of the current complex is (0.0 BM) for Au (III) complex d^8 configuration. This outcome designates a diamagnetic nature and is consistent with the square planar structure [30]. The conductivity measurement demonstrated that the complex was performing; then, the (Cl^{-1}) ion was positioned out of the coordination zone. Spectroscopy techniques analysis and data indicate a square planar geometry for this complex. The geometric shapes of the synthesis complexes can be suggested as shown in Figure 9.

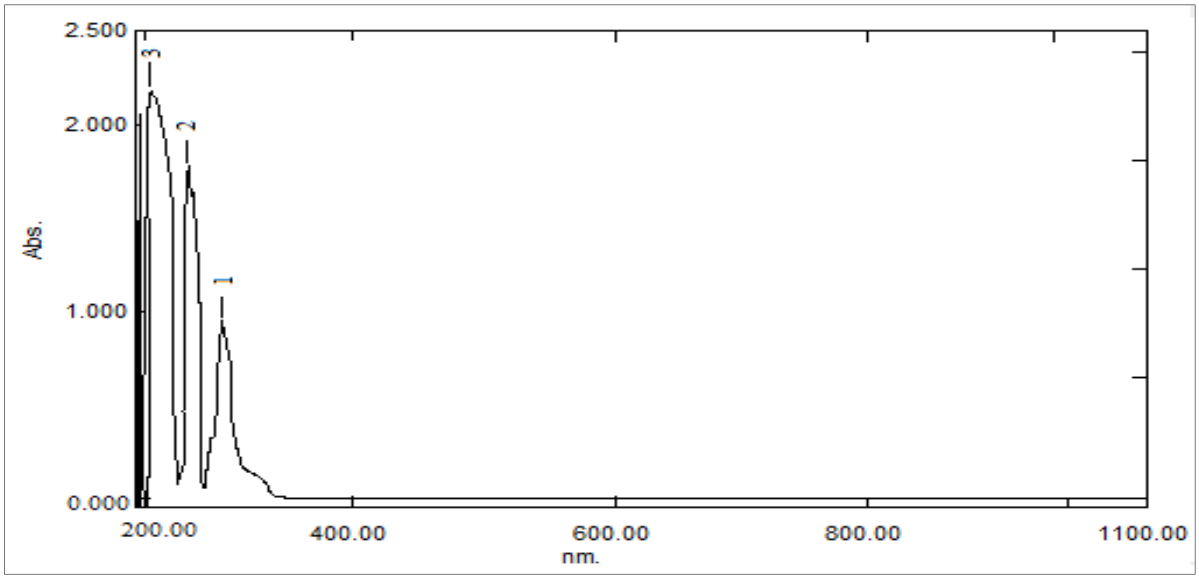

Fig. 4. L UV-Vis Spectrum.

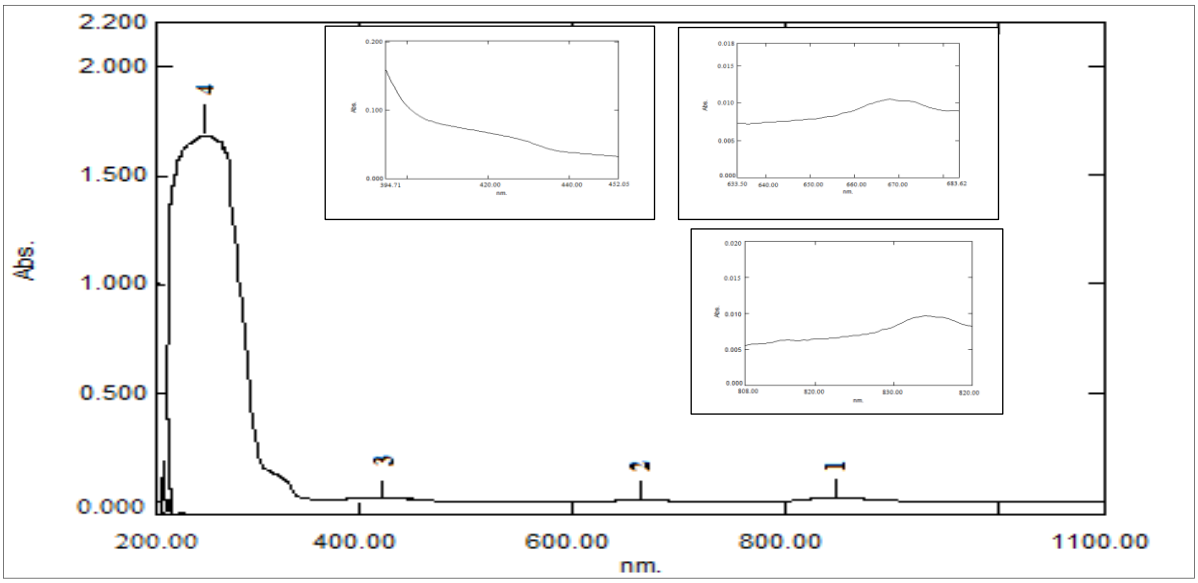

Fig. 5. VO-L UV-Vis Spectrum.

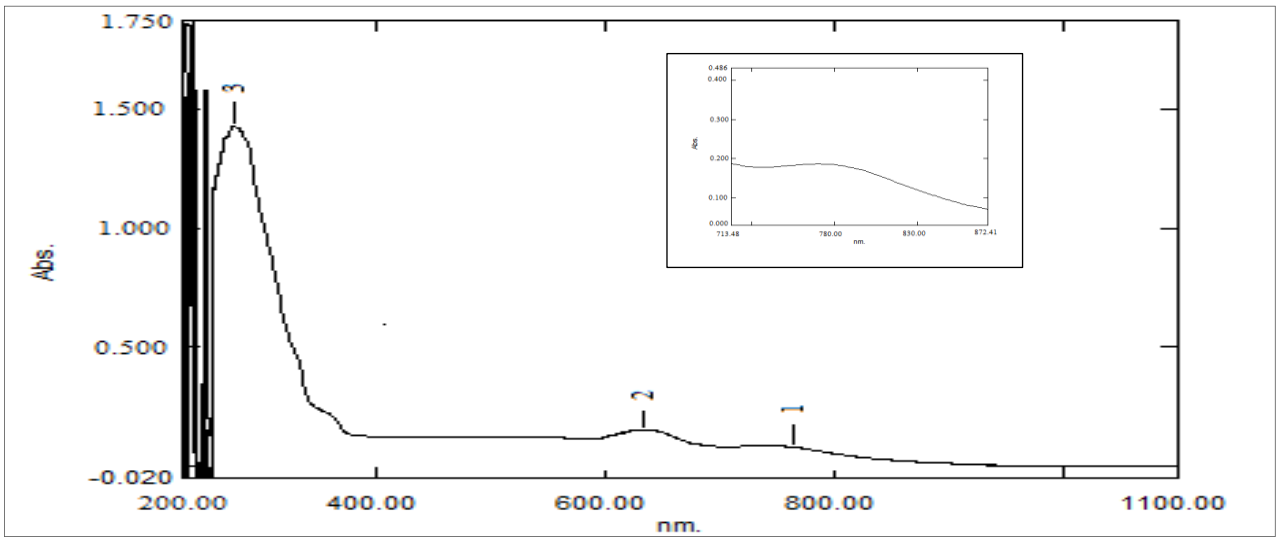

Fig. 6. Ru-L UV-Vis Spectrum.

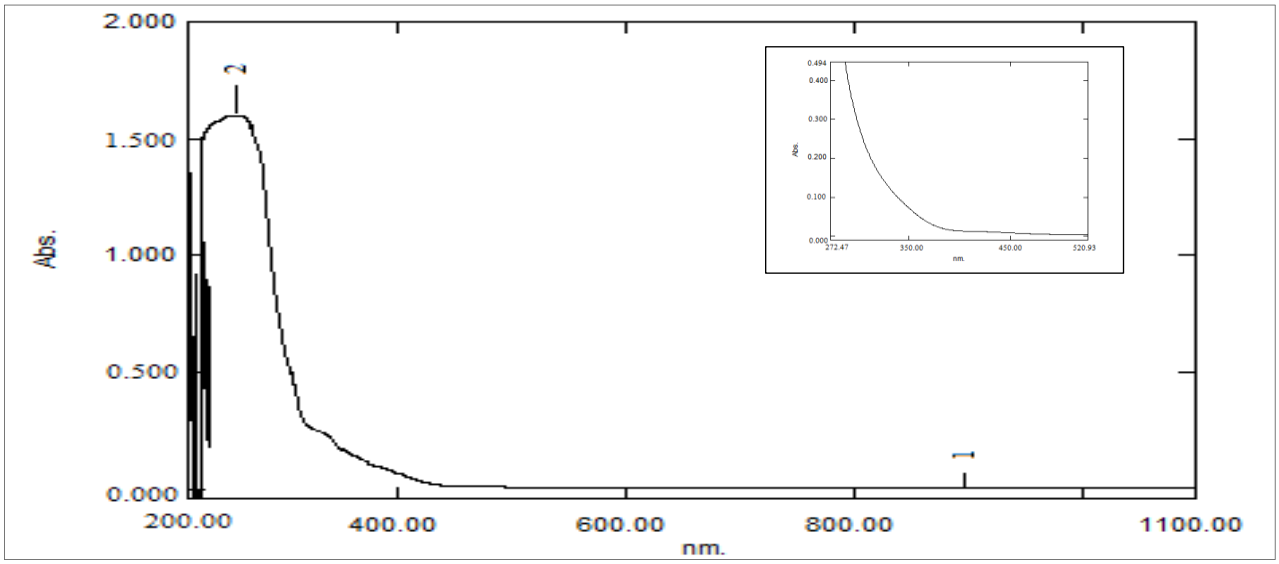

Fig. 7. Pt-L UV-Vis Spectrum.

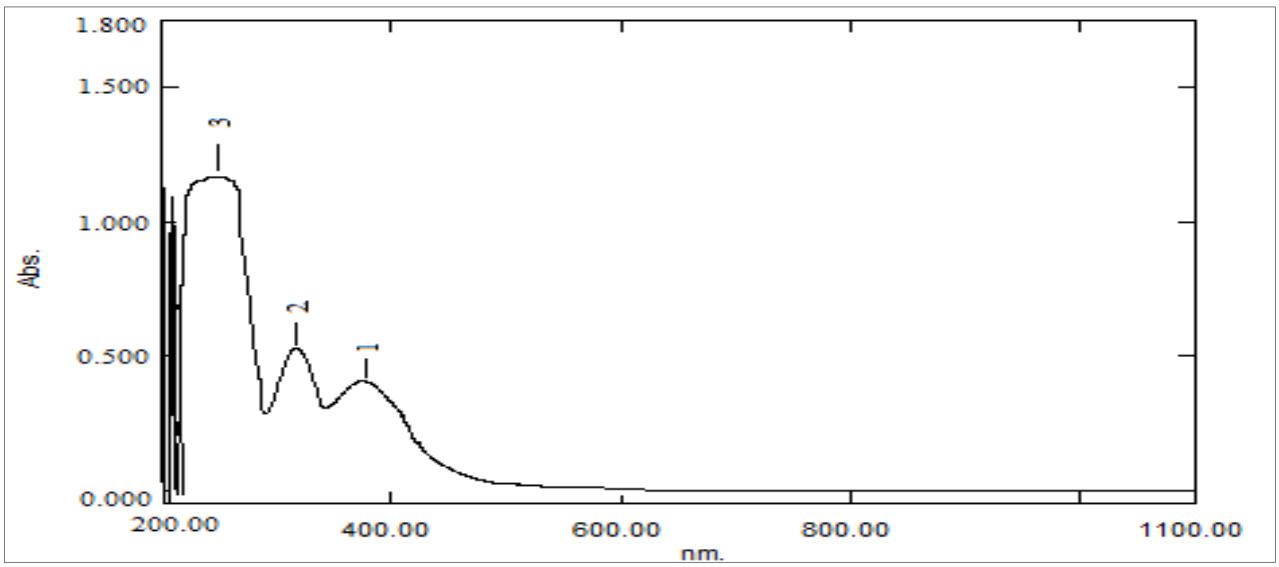

Fig. 8. Au-L UV-Vis Spectrum.

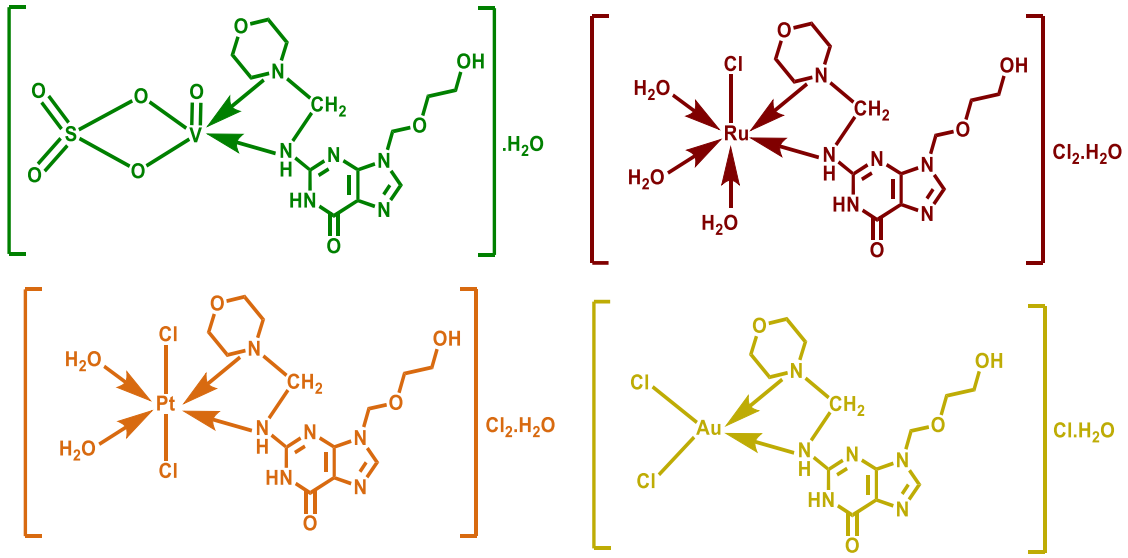

Fig. 9. Proposed geometry of synthesized complexes.

3.6. Biological Activity

3.6.1. Antioxidant Activity

Antioxidants function as neutralizing elements that mitigate oxidative damage to biological procedures by donating electrons to free radicals, thereby rendering them harmless. Free radicals are primarily related to oxidative stress.

The interaction of oxygen with certain chemicals produces free radicals, which pose a potential risk by damaging vital biological components, including DNA, proteins, and the cell membrane [31,32]. This work evaluates the DPPH scavenging activity of the Mannich base ligand and its complexes, comparing it to that of the parent molecule. The findings demonstrate that the scavenging action of these compounds was contingent upon their concentration. Among the substances evaluated, the Ru(III) complex exhibited superior activity compared to the others.

The value of IC_{50} of this combination was 311.50 µg/ml, which is less than that of the reference chemical ascorbic acid (473.15 µg/ml), indicating that the Au(III) complex displayed moderate activity. The value of IC_{50} of the Au-complex was 1219.59 µg/ml, and the ligand exhibited moderate antioxidant action. Furthermore, all compounds demonstrated reduced activity compared to the conventional ascorbic acid. The IC_{50} values of all compounds were evaluated and compared with the reference standards presented in Figure 10. The graph demonstrates the comparison of the antioxidant activity of the compounds against ascorbic acid, the recognized standard, as indicated in Table 4.

3.6.2. Antimicrobial Activity

The biological activity of these substances was evaluated. The activity assessments were conducted *in vitro* against *Acinetobacter baumannii* as Gram-negative bacterium and Streptococcus pyogenes as a Gram-positive bacterium, as well as antifungal activity against the microorganism *Candida albicans*, utilizing two separate doses (50 and 100)mg/ml of each chemical. The results indicate that, at elevated concentrations, most complexes pose a larger threat to these bacterial and fungal species than the unbound ligand.

The ligands and complexes exhibited greater resistance against a gram-positive species (*Streptococcus*) than the other microorganisms.

The enhanced activity of metal complexes can be attributed to the impact of metal ions on the cellular membrane.

Metal chelates are highly effective for cellular penetration due to their dual polar and nonpolar characteristics. Moreover, chelation can augment or diminish the metabolic potential of bioactive organic molecules [33]. The metal complexes exhibit superior antibacterial activity compared to the uncoordinated ligand and free metal ion, corroborating the literature [34].

The behavior of the compounds concerning the examined micro-organisms is associated with various factors, including the nature of the metal ions, the geometrical structure of the complexes, the arrangement of the ligands around the metal ions, the chelation effect of the organic molecules acting as ligands, the characteristics of the atoms coordinating with the metals, and the type and oxidation state of the metals involved. The findings demonstrated that the synthesized complexes showed superior activity to their ligand, with increased activity noted at higher concentrations. The Pt complex demonstrated a more synergistic effect, and the compounds acted as strong antibacterial agents against *Streptococcus (pyogenes)* at a concentration of 100 mg/ml. The results are displayed in Figure 11.

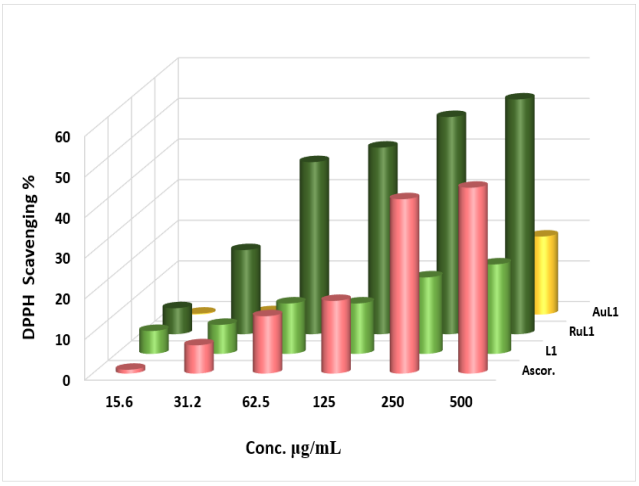

Fig. 10. DPPH scavenging activity for the ligand and its complexes.

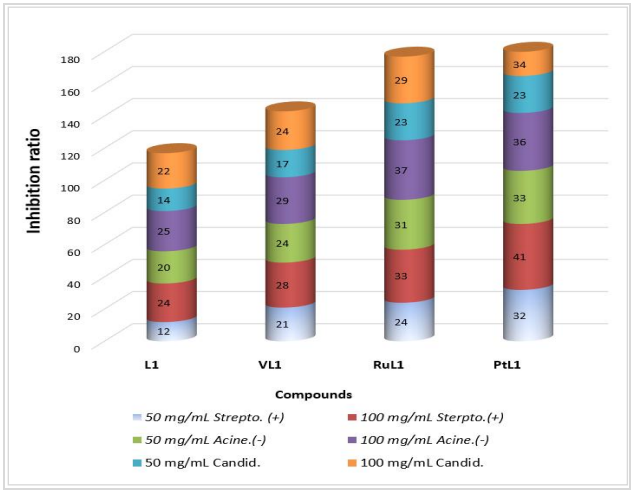

Fig. 11. Antimicrobial activity for L and its selected metal complexes against *Streptococcus (pyogenes*), *Acinetobacter (Baumann)* & *Candida albicans*.

Table 4. Scavenging activity of the ligand and its Complexes.

Comp.	Concentrations (µg/ml)						Linear eq.	R^2	IC_{50}
	15.6	31.2	62.5	125	250	500			
Ascorbic acid	0.94	6.96	14.12	17.89	42.93	45.76	y = 0.0924x + 6.2805	0.8377	473.15
L	5.64	7.15	12.42	12.42	18.83	22.03	y = 0.0319x + 7.8423	0.8565	1321.55
Ru-L	6.4	20.71	42.37	45.95	53.48	57.81	y = 0.0828x + 24.207	0.5852	311.50
Au-L	0.22	0.57	0.9	1.88	11.86	19.2	y = 0.0419x - 1.1012	0.9597	1219.59

4. Conclusion

The outcomes from the spectral and physical analysis demonstrated that the synthesis of 9-((2-hydroxyethyl) methyl)-2-((morpholino-methyl)amino)-1,9-dihydro-6H- purine-6-one and its complexes with selected metals (V^{+4}, Ru^{+3}, Pt^{+4}, and Au^{+3}) was successful. All the synthesized complexes exhibit electrical conductivity, with the exception of the Vanadyl complex. The proposed geometries include octahedral for the Ru and Pt complexes, square planar for the Au complex, and square pyramidal for the V complex. The ligand and its complexes were utilized as antimicrobial agents against the microbial [*Acinetobacter baumannii, Streptococcus pyogenes*, and *Candida albicans*], using two concentrations (50 and 100) gm/ml of each compound. The findings suggest that the synthesized complexes exhibit greater activity than their ligand, with increased activity observed alongside rising concentrations. The platinum complex exhibited a notably synergistic effect, with the compounds demonstrating significant antibacterial activity against *Streptococcus pyogenes* at a concentration of 100 mg/ml. The antioxidant analysis indicated that the Ru (III) complex exhibited superior activity compared to the others. The IC_{50} value of this complex was determined to be 311.50 µg/ml, notably lower than that of the standard compound ascorbic acid, recorded at 473.15 µg/ml.

Supplementary files

Supplementary file 1.

References

[1] (a) E. Hemmati, S. Soleimani-Amiri, M. Kurdtabar, A CMC-*g*-poly(AA-co-AMPS)/Fe_3O_4 hydrogel-nanocomposite as a novel biopolymer-based catalyst in the synthesis of 1,4-dihydropyridines. *RSC Advs.*, 13(24) (2023) 16567-16583. https://doi.org/10.1039/D3RA01389H; (b) S. Soleimani Amiri, M. Ghazvini, S. Khandan, S. Afrashteh, KF/Clinoptilolite@MWCNTs Nanocomposites Promoted a Novel Four-Component Reaction of Isocyanides for the Green Synthesis of Pyrimidoisoquinolines in Water. *Polycycl. Aromat. Comp.*, 42(7) (2022) 4736-4751. https://doi.org/10.1080/10406638.2021.1912122; (c) M. Kurdtabar, S. Soleimani-Amiri, M. Alidad, G. Bagheri Marandi, Cu-Decorated CMC-*g*-PAA/Fe_3O_4 Hydrogel Nanocomposite: High Efficiency and Reusable Catalyst for Synthesis of 1,2,3-Triazoles via Click Reaction in Water. *J. Polym. Environ.*, 33(5) (2025) 2334–2350. https://doi.org/10.1007/s10924-025-03536-1; (d) N. Nasehi, B. Mirza, S. Soleimani-Amiri, Experimental and Theoretical Investigation on Imidazole Derivatives Using Magnetic Nanocatalyst: Green Synthesis, Characterization, and Mechanism Study. *Polycycl. Aromat. Comp.*, 43(9) (2023) 7890-7911. https://doi.org/10.1080/10406638.2022.2141275.

[2] (a) E. Askari, A. Alborzi, Ammonium Iron(III) Sulfate as an Eco-friendly Catalyst for the Synthesis of Spirooxindole Dihydroquinazolinone Derivatives. *J. Chem. Technol.*, 1(2) (2025) 85–89. https://doi.org/10.22034/jchemtech.2025.538321.1014; (b) B. S. Hirani, S. B. Gurubaxani, The multifaceted potential of thiazole derivatives: Robust synthesis techniques and their biological activities. Med. Med. Chem., 2(2) (2025) 92–97. https://doi.org/10.22034/medmedchem.2025.514812.1031; (c) E. Kanaani, M. Nasr-Esfahani, M. Montazerozohori, Citrate trisulfonic acid as a novel, recyclable, and heterogeneous organocatalyst for the one-pot synthesis of 4-iminoquinolines. J. Chem. Lett., 4(3) (2023) 156–163. https://doi.org/10.22034/jchemlett.2023.413639.1134; (d) S. S. Khaleel, A. Waleed, A. Hassen, Synthesis and characterization of some thiazole rings derived from theophylline and study of their antibacterial activity. Chem. Rev. Lett. 8(4) (2025) 849-855. https://doi.org/10.22034/crl.2025.488938.1475.

[3] S. K. Raju, A. Settu, A. Thiyagarajan, D. Rama, Synthetic applications of biologically important Mannich bases: An updated review. *Open Acc. Res. J. Bio. Pharm.* 7(2) (2023) 1-15. https://doi.org/10.53022/oarjbp.2023.7.2.0015

[4] N. V. Bhilare, V. S. Marulkar, P. J. Shirote, S. A. Dombe, V. J. Pise, P. L. Salve, S. M. Biradar, V. D. Yadav, P. D. Jadhav, A. A. Bodhe, S. P. Borkar, Mannich bases: centrality in cytotoxic drug design. *Medic. Chem.* 18(7) (2022) 735-756. https://doi.org/10.2174/1573406418666211220124119.

[5] A. M. Abdula, A. F. Qarah, K. Alatawi, J. Qurban, M. M. Abualnaja, H. A. Katuah, N. M. El-Metwaly, Design, synthesis, and molecular docking of new phenothiazine incorporated N-Mannich bases as promising antimicrobial agents. *Hel.* 10(7) (2024) 1-13.https://doi.org/10.1016/j.heliyon.2024.e28573.

[6] (a) L. Cicco, G. Dilauro, F. M. Perna, P. Vitale, V. Capriati, Advances in deep eutectic solvents and water: applications in metal-and biocatalyzed processes in the synthesis of APIs, and other biologically active compounds. Org. Biomol. Chem. 19(12) (2021) 2558-2577. https://doi.org/10.1039/D0OB02491K; (b) R. C. DiPucchio, S. C. Rosca, L. L. Schafer, Hydro amino alkylation for the catalytic addition of amines to alkenes or alkynes: diverse mechanisms enable diverse substrate scope. *J. Amer. Chem. Soci.* 144(26) (2022) 11459-11481. https://doi.org/10.1021/jacs.1c10397; (c) D. Sriram, P. Yogeeswari, S. P. Reddy, Synthesis of pyrazinamide Mannich bases and its antitubercular properties. *Bioorg. Medic. Chem. Lett.* 16(8) (2006) 2113-2116. https://doi.org/10.1016/j.bmcl.2006.01.064.

[7] V. V. Kouznetsov, Exploring acetaminophen prodrugs and hybrids: a review. *RSC adv.* 14(14) (2024) 9691-9715.https://doi.org/10.1039/D4RA00365A.

[8] E. J. Waheed, A. Al-Khazraji, A. A. Ahmed, Versatile applications of mannich base ligands and their metal complexes: a review article. *J. App. Sci. Nano.* 3(4) (2023) 42-61. https://doi.org/10.53293/jasn.2023.7033.1228.

[9] M. Ramasamy, G. Velayutham, R. Pitchaipillai, A Novel Mannich Based Metal II Complexes: Synthesis and Characterization of Magnetic, Conductivity and Antimicrobial Properties. *Eurasian J. Anal. Chem.* 30(1) (2025) 60-75. https://doi.org/10.31489/2959-0663/1-25-5.

[10] F. S. Jaafar, M. F. Alias, Chemistry of Metalloguanines: An Overview of Their Synthesis Routes and Their Implementations for the Period 2000-2024. *Karbala Inter. J. Modern Sci.* 11(1) (2025) 1-12. https://doi.org/10.33640/2405-609X.3392.

[11] S. S. Raoof, A. S. Sadiq, Mannich bases: Synthesis, pharmacological activity, and applications: A review. *Iraqi J. Sci.* 63(12) (2022) 5086-5105. https://doi.org/10.24996/ijs.2022.63.12.1.

[12] Joshi S, Bilgaiyan P, Pathak A. Synthesis and in-vitro study of some medicinally important mannich bases derived from 2-amino-9 [{(1, 3 dihydroxy propane-2yl) oxy} methyl] 6-9 dihydro-3h-purin-6-one. *J. Chil. Chem. Soci.* 57(3)(2012)1277-1282. http://dx.doi.org/10.4067/S0717-97072012000300017.

[13] Joshi S, Bilgaiyan P, Pathak A. Synthesis, spectroscopic characterization and antibacterial screening of novel Mannich bases of Ganciclovir. *Arabian J. Chem.* 10 (2017) 1180-1187. http://dx.doi.org/10.1016/j.arabjc.2013.02.013.

[14] E. O. AlTamiemi, S. J. Khammas, S. S. AlKaissi, Synthesis and Characterization of Some New Morpholine Derivatives. *Baghdad Sci. J.* 13(2) (2016) 253-253. https://doi.org/10.21123/bsj.2016.13.2.2NCC.0253.

[15] T. J. Hossain, Methods for screening and evaluation of antimicrobial activity: A review of protocols, advantages, and limitations. *Eur. J. Microbiol. Immunol.* 14(2) (2024) 97-115. https://doi.org/10.1556/1886.2024.00035.

[16] İ. Öztürk, N. Beğiç, M. Bener, R. Apak, Antioxidant capacity measurement based on κ-carrageenan stabilized and capped silver nanoparticles using green nanotechnology. *J. Mol. Struc.* 1242 (2021) 1-12. https://doi.org/10.1016/j.molstruc.2021.130846.

[17] D. Kowalczuk, A. Gładysz, M. Pitucha, D. M. Kamiński, A. Barańska, B. Drop, Spectroscopic study of the molecular structure of the new hybrid with a potential two-way antibacterial effect. *Mol.* 26(5) (2021) 1-16. https://doi.org/10.3390/molecules26051442.

[18] H. H. Mihsen, S. K. Abass, Z. M. Hassan, A. K. Abass, Synthesis, characterization and antimicrobial activities of mixed ligand complexes of Fe (II), Co (II), Ni (II) and Cu (II) ions derived from imine of benzidine and o-phenylenediammine. *Iraqi J. Sci.* 61(11) (2020) 2762-2775. https://doi.org/10.24996/ijs.2020.61.11.2.

[19] F. S. Jaafar, M. F. Alias, Application of Benesi–Hildebrand and Tauc approaches of new synthesized Schiff bases interacted with two types of electron acceptors modules. *J. Umm Al-Qura Univ. App. Sci.* 11(2) (2025) 1-21. https://doi.org/10.1007/s43994-025-00243-4

[20] B. H. Stuart, Infrared spectroscopy: fundamentals and applications. John Wiley & Sons (2004). https://onlinelibrary.wiley.com/doi/book/10.1002/0470011149.

[21] S. R. Bakir, Synthesis, spectral studies, and theoretical treatment of some new metal complexes with tridentate ligand (Schiff and Mannich Base). *Baghdad Sci. J.* 13(2) (2016) 340-351. https://doi.org/10.21123/bsj.2016.13.2.0340

[22] E. Yousif, A. Majeed, K. Al-Sammarrae, N. Salih, J. Salimon, B. Abdullah, Metal complexes of Schiff base: preparation, characterization and antibacterial activity. *Arabian J. Chem.* 10 (2017) 1639-1644. https://doi.org/10.1016/j.arabjc.2013.06.006

[23] B. N. Figgis, M. A. Hitchman, Ligand field theory and its applications, Wiley-VCH (1999).

[24] I. Ali, W. A. Wani, K. Saleem, Empirical formulae to molecular structures of metal complexes by molar conductance. *Synth. React. Inorg. Met.-Org. Chem.* 43(9) (2013) 1162-1170. https://doi.org/10.1080/15533174.2012.756898.

[25] R. A. Al-Hasani, A. H. Abed, S. K. Ibrahim, Syn-thesis, characterization, theoretical studies and bioactivity of Pd (II), Rh (III), Ru (III) and Pt (IV) complexes with 1, 8-naphthalimide derivative. *Iraqi J. Sci.* 57(4) (2016) 2575-2591. https://ijs.uobaghdad.edu.iq/index.php/eijs/article/view/6289.

[26] A. S. Alturiqi, A. N. Alaghaz, R. A. Ammar, M. E. Zayed, Synthesis, Spectral Characterization, and Thermal and Cytotoxicity Studies of Cr (III), Ru (III), Mn (II), Co (II), Ni (II), Cu (II), and Zn (II) Complexes of Schiff Base Derived from 5-Hydroxymethylfuran-2-carbaldehyde. *J. Chem.* 2018(1) (2018) 1-17.https://doi.org/10.1155/2018/5816906.

[27] W. H. Hegazy, M. Gaafar, Synthesis, characterization and antibacterial activities of new Pd (II) and Pt (IV) complexes of some unsymmetrical tetradentate Schiff bases. *Amer. Chem. Sci. J.* 2(3) (2012) 86-99. https://journalcsij.com/index.php/CSIJ/article/view/575/1149.

[28] P. A. Ajibade, G. A. Kolawole, Synthesis, characterization, antiplasmodial and antitrypanosomal activity of some metal (III) complexes of sulfadiazine. *Bull. Chem. Soc. Ethiop.* 22(2) (2008) 261-268. https://doi.org/10.4314/bcse.v22i2.61295.

[29] H. U. Abbas, R. E. AL-Hassani, Spectroscopic characterization and Bioactivty studies of new Co (II), Ni (II), Cu (II), Au (III) and Pt (IV) complexes with didentate (NO) donarazo dye ligand. *Int. J. Med. Sci. Dent. Res.* 1(1) (2018) 38-51. https://www.ijmsdr.org/pages/Volume%201%20issue1.html.

[30] M. Baron, A. Dall'Anese, C. Tubaro, L. Orian, V. Di Marco, S. Bogialli, C. Graiff, M. Basato, A square planar gold (III) bis-(1,1-dimethyl-3,3-methylene-diimidazol-2,2'-diylidene) trication as an efficient and selective receptor towards halogen anions: the cooperative effect of Au···X and X···HC interactions. *Dalt. Trans.* 47(3) (2018) 935-945. https://doi.org/10.1039/C7DT03672H.

[31] S. Baliyan, R. Mukherjee, A. Priyadarshini, A. Vibhuti, A. Gupta, R. P. Pandey, C. M. Chang, Determination of antioxidants by DPPH radical scavenging activity and quantitative phytochemical analysis of Ficus religiosa. *Mol.* 27(4) (2022) 1-19. https://doi.org/10.3390/molecules27041326.

[32] I. S. Hamza, R. K. Al-Daffaay, S. S. Faris, A. A. Al-Hamdani, Ru^{+3}, Rh^{+3}, Pd^{+2}, Pt^{+4} and Au^{+3} Metal ions Complexes with Azo Derived from 4-Aminomethyl-cyclohexane carboxylic acid Synthesis, Characterization, Thermal Study and Antioxidant Activity. *Iraqi J. Sci.* 66(3) (2025) 1010-1024. https://doi.org/10.24996/ijs.2025.66.3.3.

[33] J. Devi, S. Kumar, B. Kumar, S. Asija, A. Kumar, Synthesis, structural analysis, in vitro antioxidant, antimicrobial activity and molecular docking studies of transition metal complexes derived from Schiff base ligands of 4-(benzyloxy)-2-hydroxybenzaldehyde. *Res. Chem. Intermed.* 48(4) (2022) 1541-1576. https://doi.org/10.1007/s11164-021-04644-y.

[34] B. Sharma, S. Shukla, R. Rattan, M. Fatima, M. Goel, M. Bhat, S. Dutta, R. K. Ranjan, M. Sharma, Antimicrobial agents based on metal complexes: present situation and future prospects. *Int. J. Biomater.* 2022(1) (2022) 1-21. https://doi.org/10.1155/2022/6819080.